Thermometry at Low Temperatures

- Magnetic susceptibility
- Current-sensing noise thermometer CSNT
- Cross-correlated current noise thermometer C3NT
- Magnetic flux fluctuation thermometer MFFT
- Shot-noise thermometer

First SQUID-based noise thermometer in 1971

testet and demonstrated for: 1.4 K < *T*< 4 K.

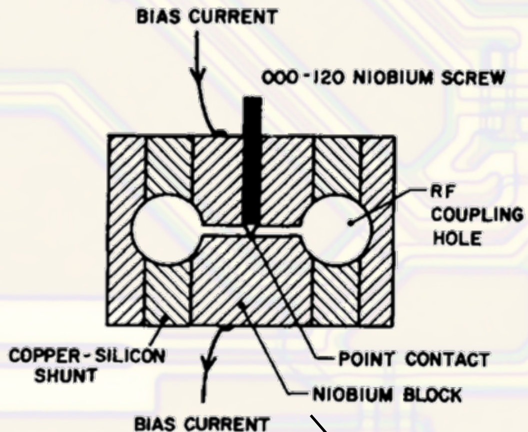

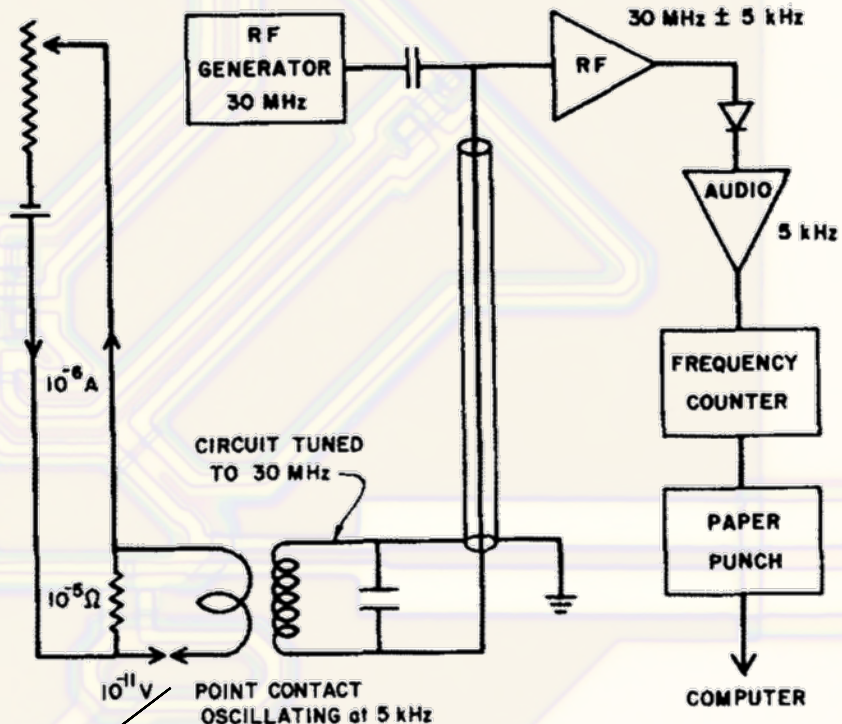

rf-SQUID

Thermometry at Low Temperatures

Noise thermometer

thermal voltage fluctuations across a conductor (predicted by A. Einstein 1905)

1927

John Bertrand "Bert" Johnson

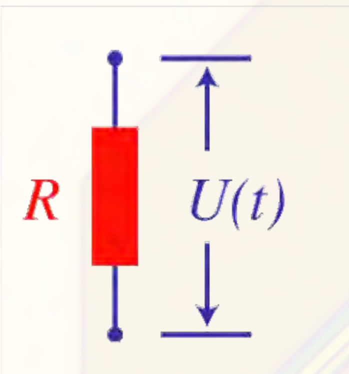

power spectral density

$$S_U = \frac{\langle U^2 \rangle}{\Delta f} = 4 k_B T R$$

1928

Harry Nyquist

quantum corrections $$S_U = \frac{\langle U^2 \rangle}{\Delta f} = 4 h f R \left[\frac{1}{2} + \frac{1}{e^{hf/k_B T} - 1} \right]$$

for $hf/k_B T \ll 1$ $$\approx 4 k_B T R \left[1 + \frac{1}{12} \frac{hf}{k_B T} \right]$$

can be neclegted since
(T > 100 µK, f < 1 kHz) $$\frac{hf}{k_B T} < 5 \times 10^{-4}$$

Thermometry at Low Temperatures

Current-sensing noise thermometer

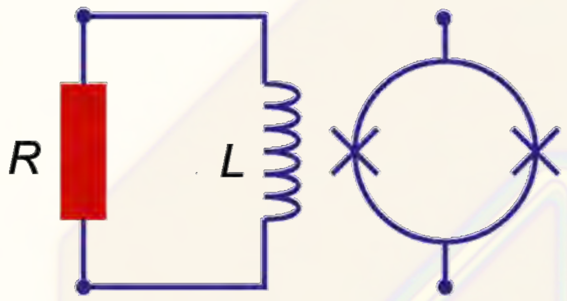

current noise $S_I = \dfrac{\langle I^2 \rangle}{\Delta f} = \dfrac{4k_\mathrm{B}T}{R}$

For $R \sim$ mΩ even at $T \sim$ 1 mK large, compared to SQUID current sensitivity

Finite bandwidth due to reactance $i\omega L$:

$$S_I = \frac{\langle I^2 \rangle}{\Delta f} = \frac{4k_\mathrm{B}T}{R}\,\frac{1}{1+(f/f_0)^2}$$

$$f_0 = (1/2\pi)L/R$$

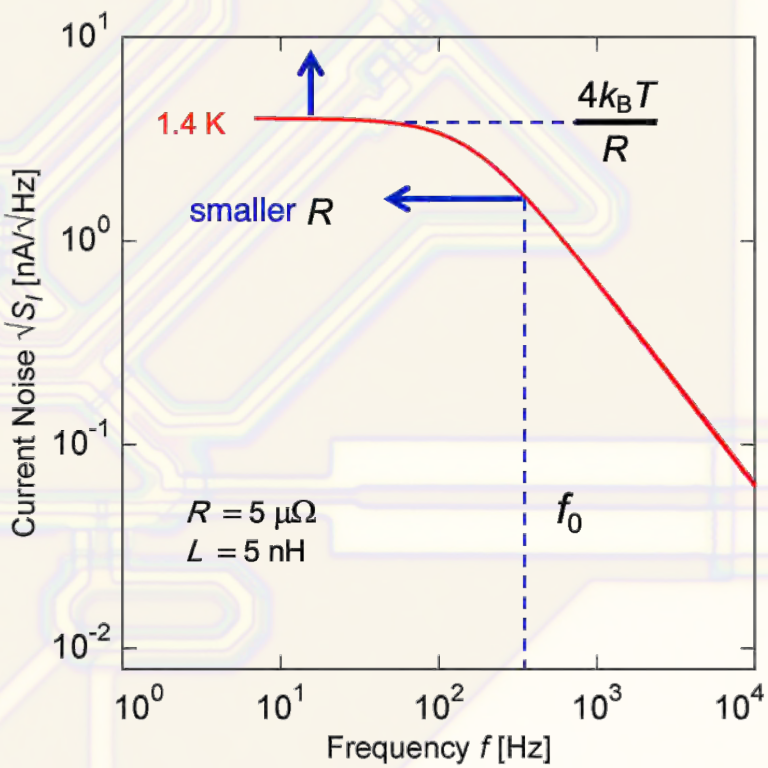

Coil = one degree of freedom, thus

$$\overline{E} = \int_0^\infty \frac{1}{2}\,L\,S_I\,\mathrm{d}f = \frac{1}{2}k_\mathrm{B}T$$

Current-sensing noise thermometer

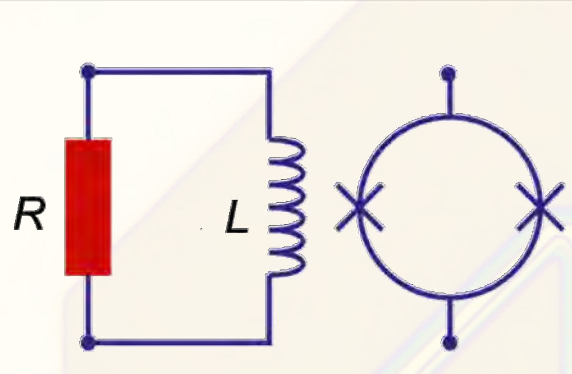

current noise $S_I = \frac{\langle I^2 \rangle}{\Delta f} = \frac{4 k_\mathrm{B} T}{R}$

For $R \sim$ mΩ even at $T \sim 1$ mK large, compared to SQUID current sensitivity

Finite bandwidth due to reactance $i\omega L$:

$$S_I = \frac{\langle I^2 \rangle}{\Delta f} = \frac{4 k_\mathrm{B} T}{R} \frac{1}{1 + (f/f_0)^2}$$

$$f_0 = (1/2\pi) L/R$$

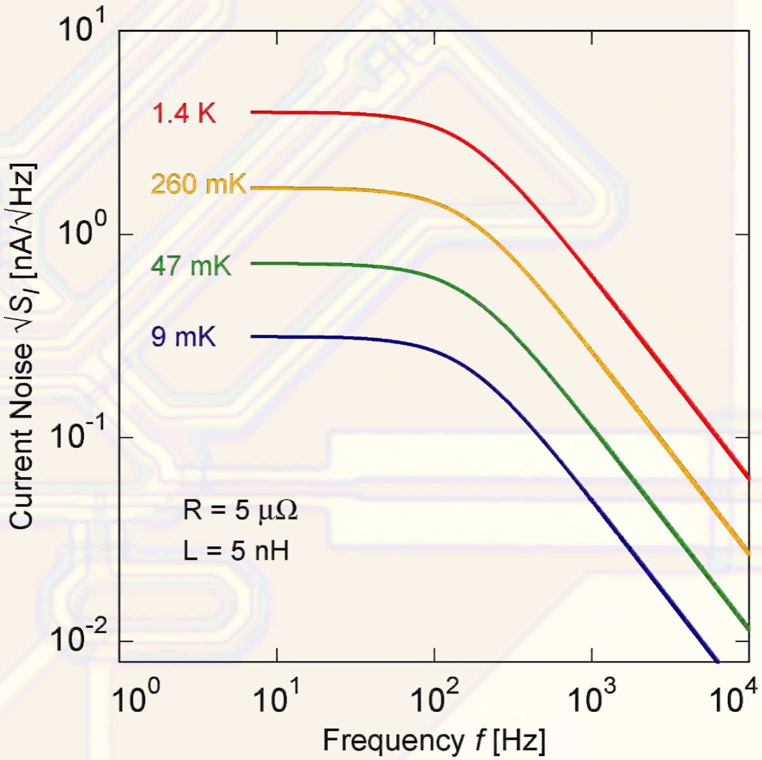

Coil = one degree of freedom, thus

$$\overline{E} = \int_0^\infty \frac{1}{2} L\, S_I \, \mathrm{d}f = \frac{1}{2} k_\mathrm{B} T$$

Thermometry at Low Temperatures

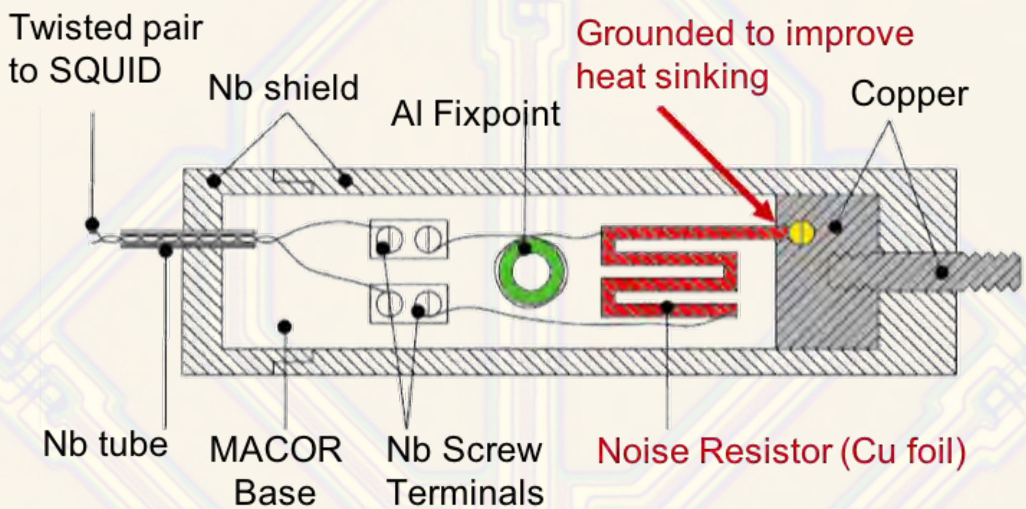

Readout

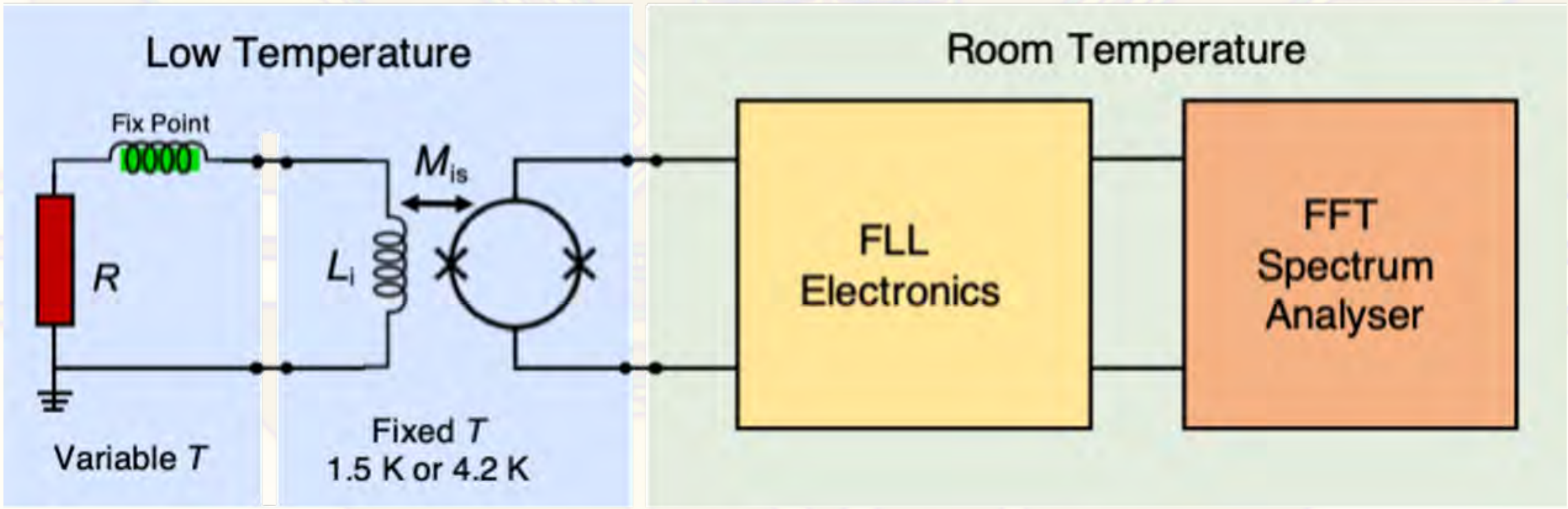

Thermometry at Low Temperatures

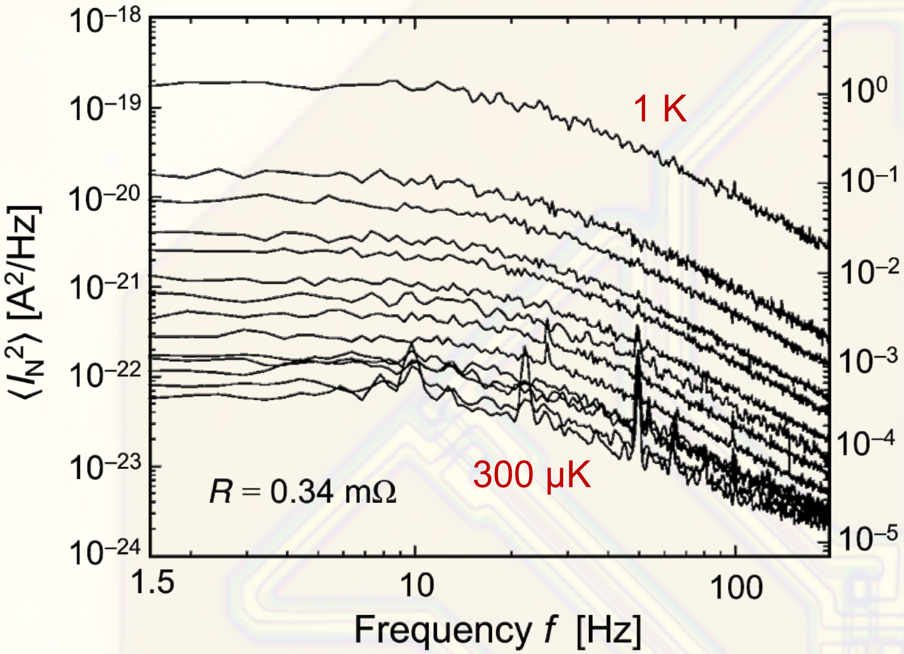

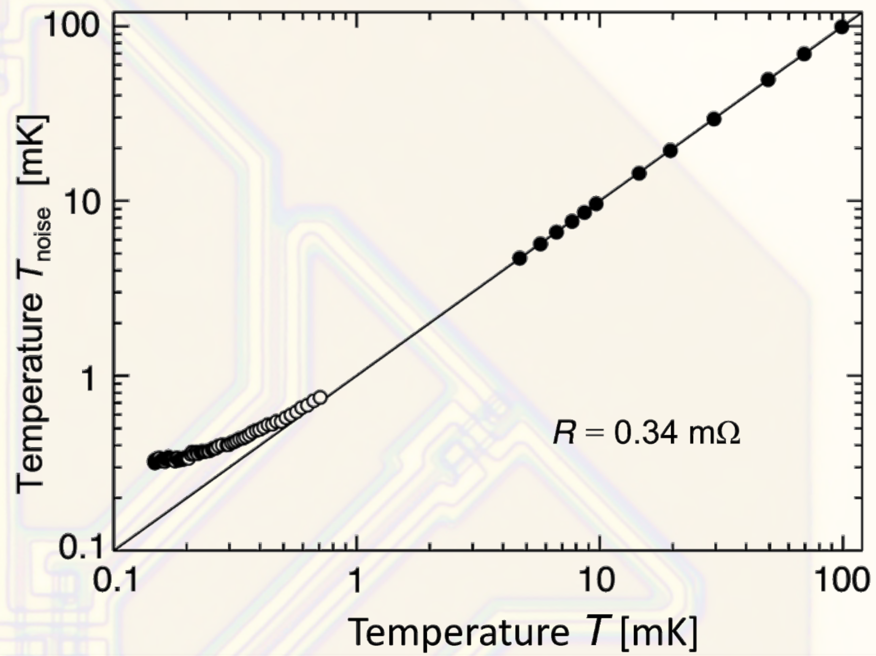

^{3}He melting curve thermometer (PTB), Pt-NMR and calibrated resistance thermometers

- lowest noise power corresponds to: $T = 300\ \mu K$
- Decoupling caused by parasitic heat flow of few pW through the 0.3 mΩ resistor

Cross-Correlated Current Noise Thermometer

C3NT

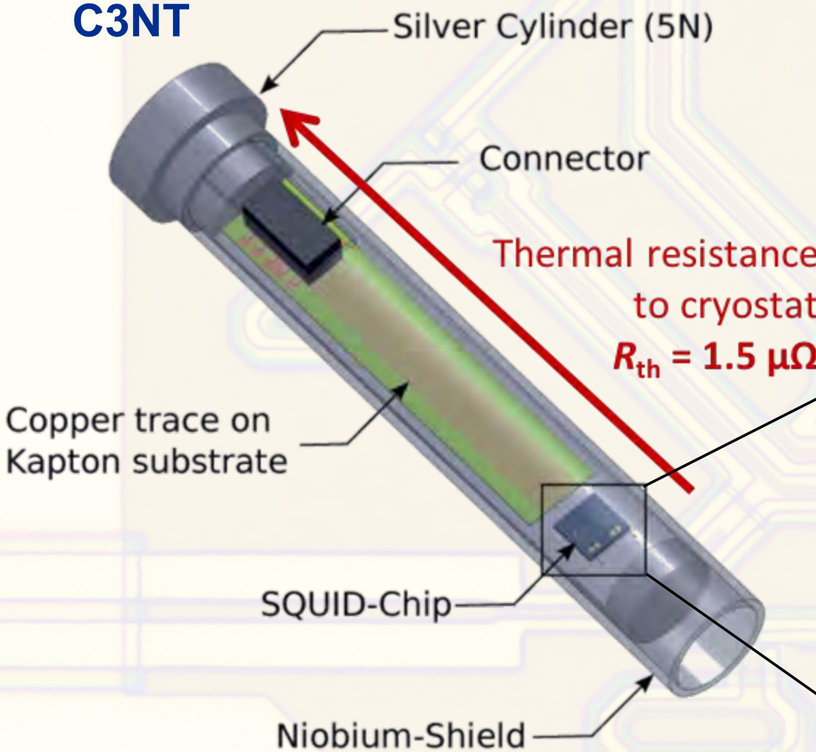

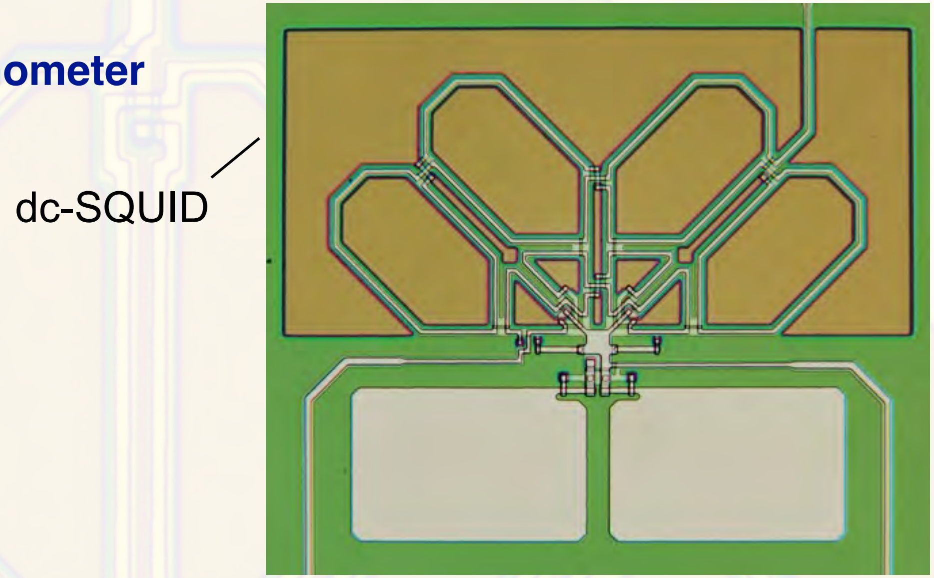

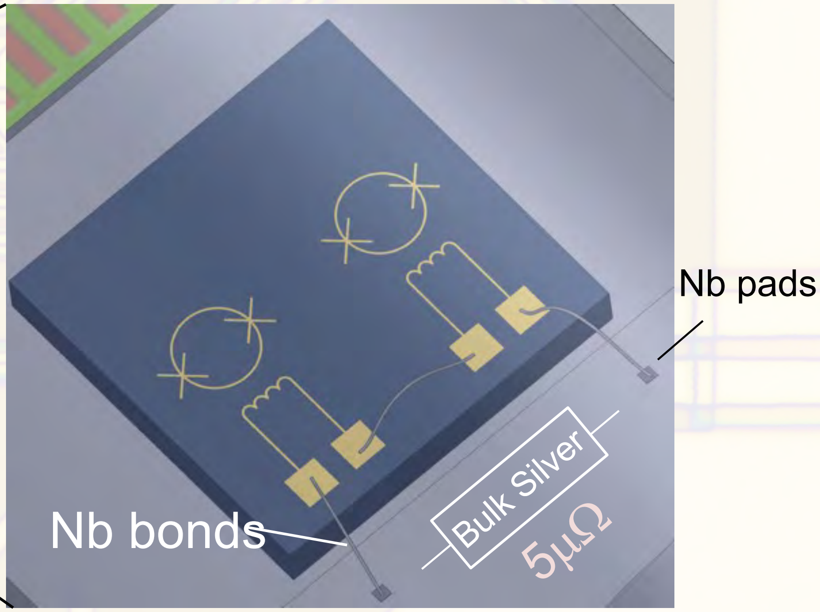

Thermometry at Low Temperatures

Readout with Cross-Correlation

- signal measured in two channels
- suppression of uncorrelated amplifier noise by cross-correlation

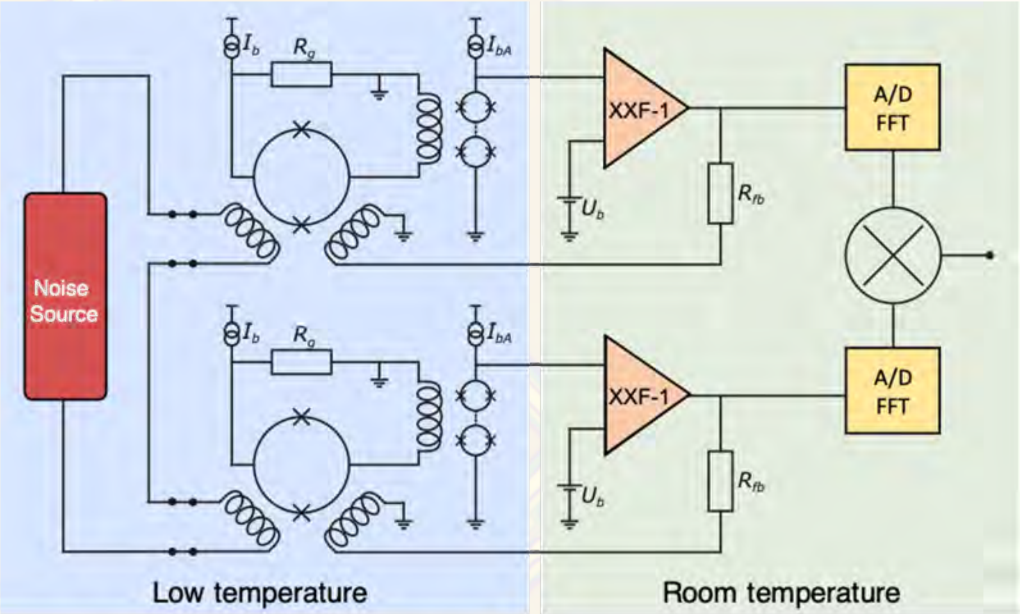

Channel 1: $A_1(t) = U(t) + N_1(t)$

Channel 2: $A_2(t) = U(t) + N_2(t)$

if $U(t), N_1(t), N_2(t)$ pairwise uncorrelated

Cross Correlation:

$$C(t') = \lim_{T_W \to \infty} \frac{1}{T_W} \int_0^{T_W} A_1(t) A_2(t+t') \mathrm{d}t \overset{\downarrow}{=} R(t)$$

Auto Correlation

Spectral Power Density via Wiener-Khinchin Theorem

$$S(\omega) = 2 \int_{-\infty}^{\infty} R(t)\, \mathrm{e}^{-i\omega t} \mathrm{d}t$$

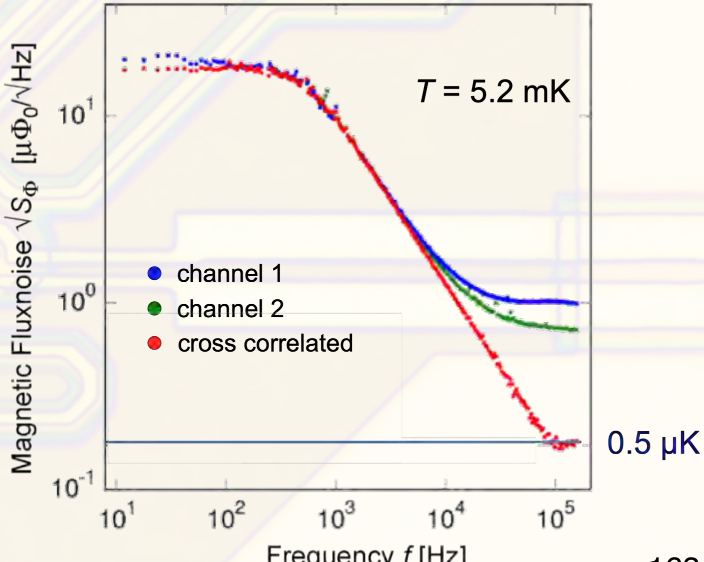

Thermometry at Low Temperatures

Noise spectra at different temperatures

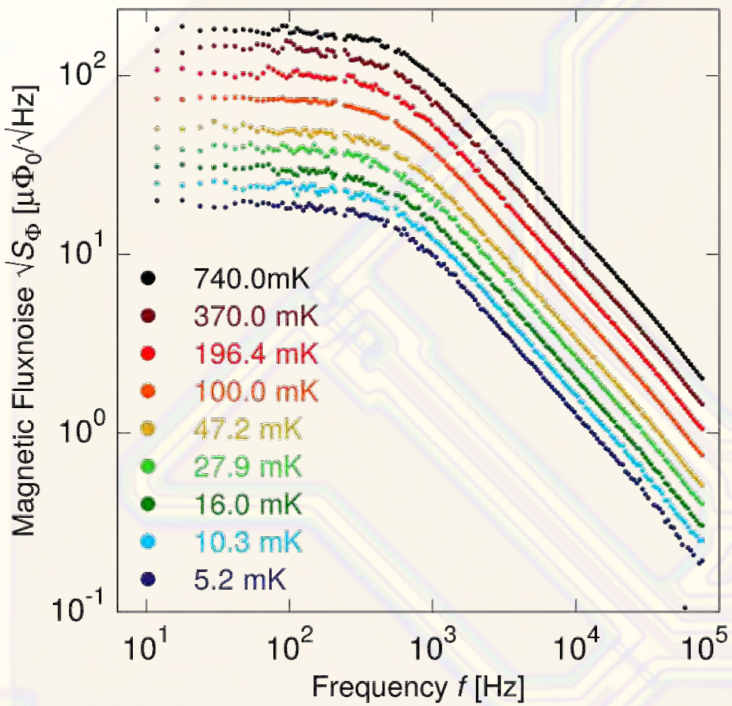

C3NT vs MFFT

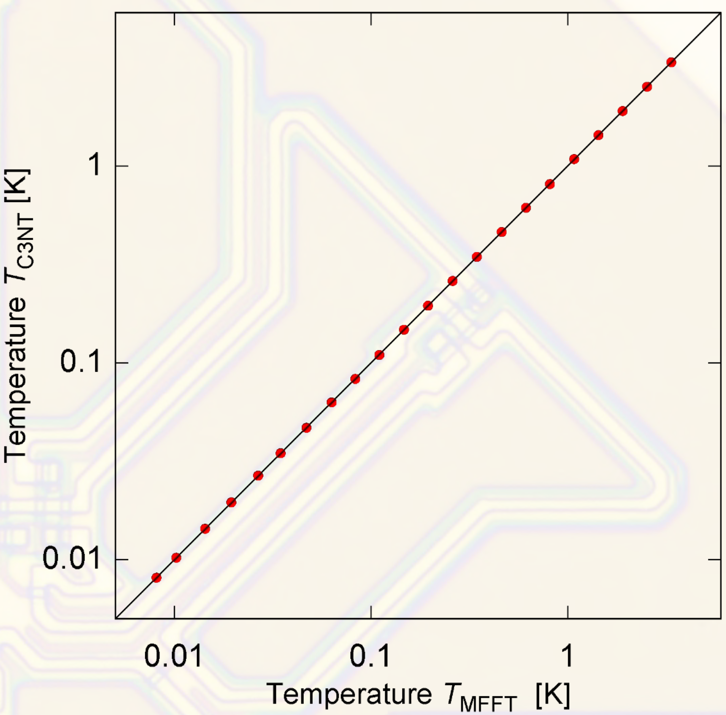

- ► no change of spectral form
- ► agreement between thermometers better than 0.3% after 35 s
- ► deviations purely of statistical nature

Thermometry at Low Temperatures

Expected statistical uncertainty:

$$\frac{\Delta T}{T} = \frac{\sqrt{2}}{\sqrt{\underbrace{\Delta f}_{\text{bandwidth}} \underbrace{\Delta t}_{\text{measuring time}}}}$$

Deviations between C3NT and MFFT

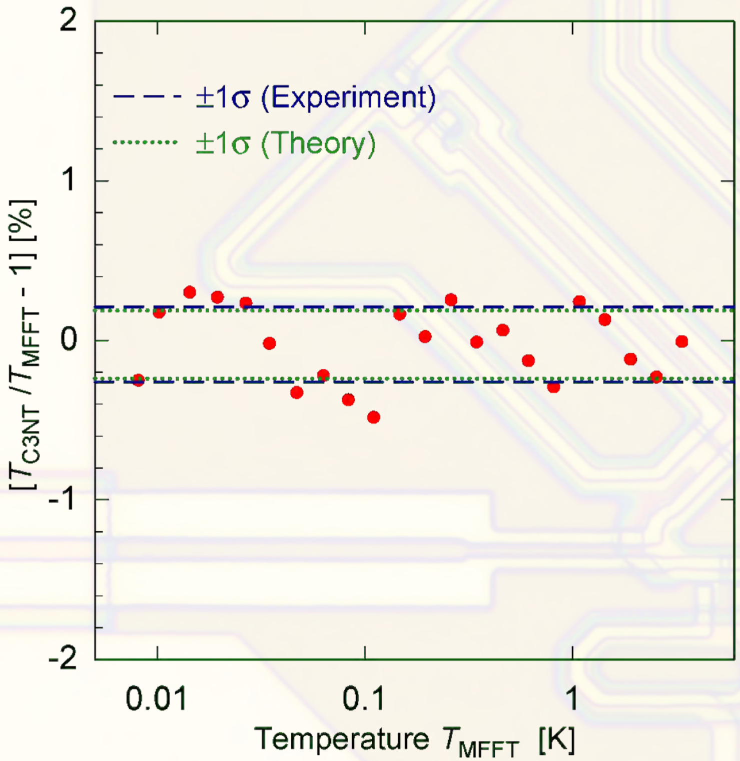

Statistical uncertainty vs measurement time

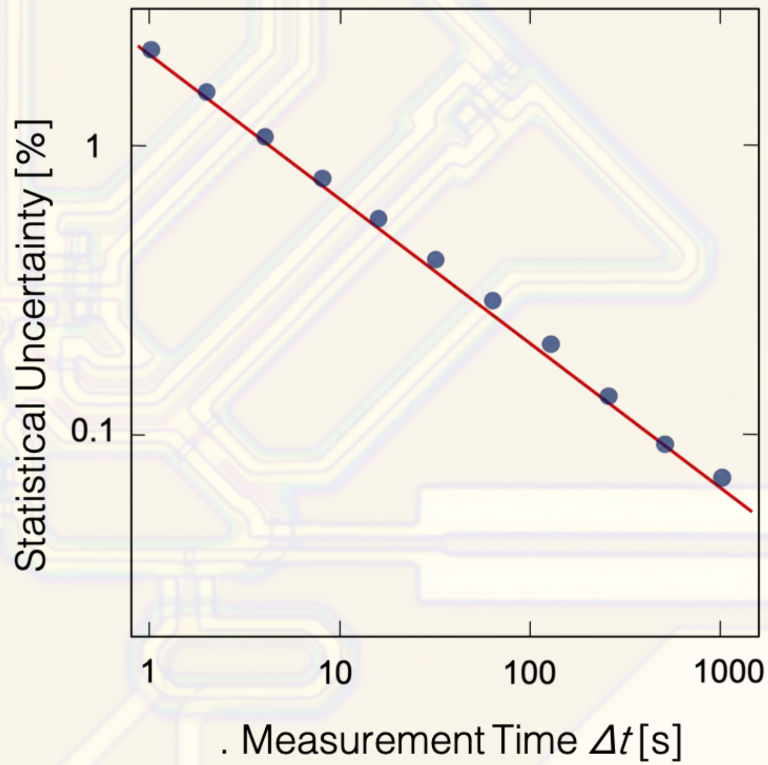

Magnetic Flux Fluctuation Thermometer

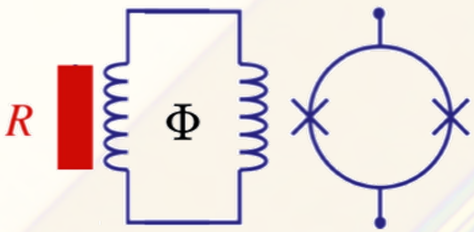

$Z = R(\omega) + i\omega L(\omega)$

flux noise $$S_\Phi(f,T) = \frac{4k_\mathrm{B}T\Re(Z(f))}{(2\pi f)^2}$$

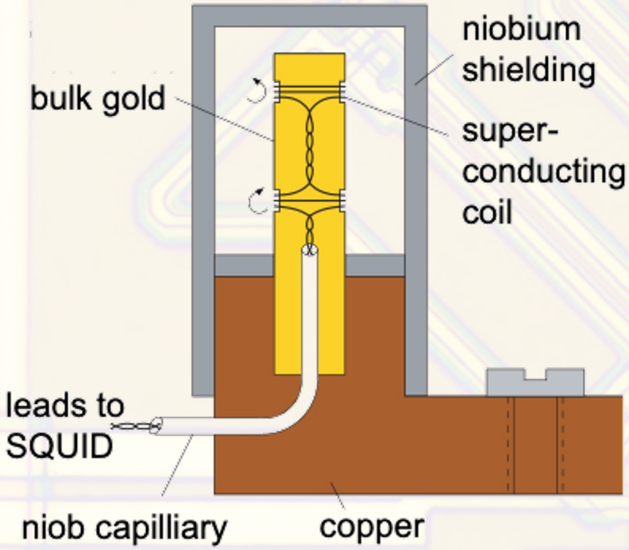

$f_\mathrm{c} \simeq 4.5/(\pi\mu_0\sigma r^2)$

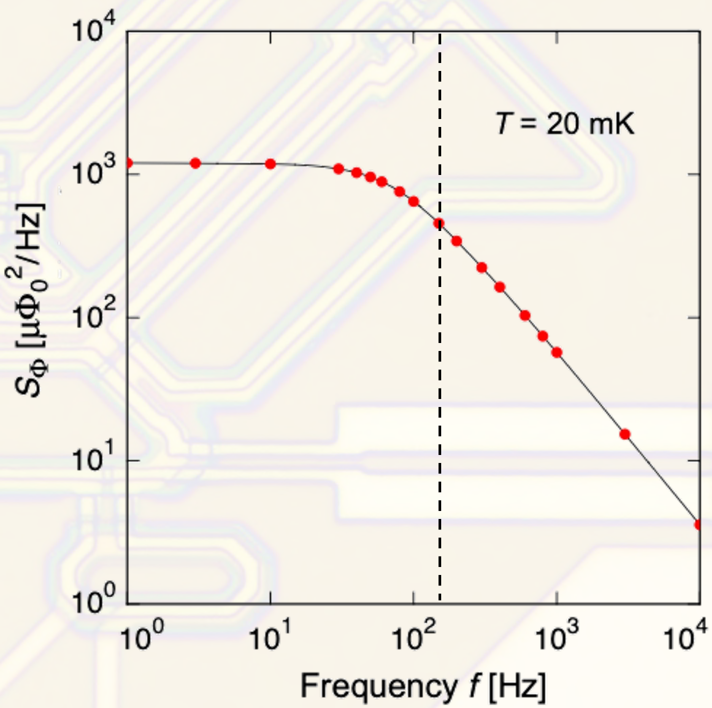

Noise source :

Gold cylinder ∅ 2 mm
purity > 99,999%, RRR = 110

Thermometry at Low Temperatures

Noise spectra at different temperatures

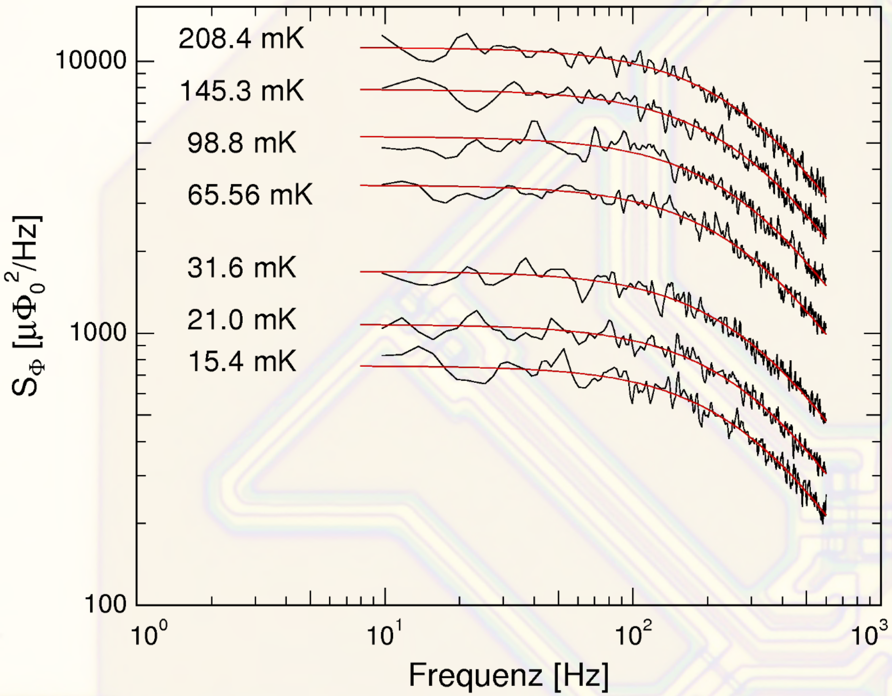

S_Φ vs temperature fix point scale

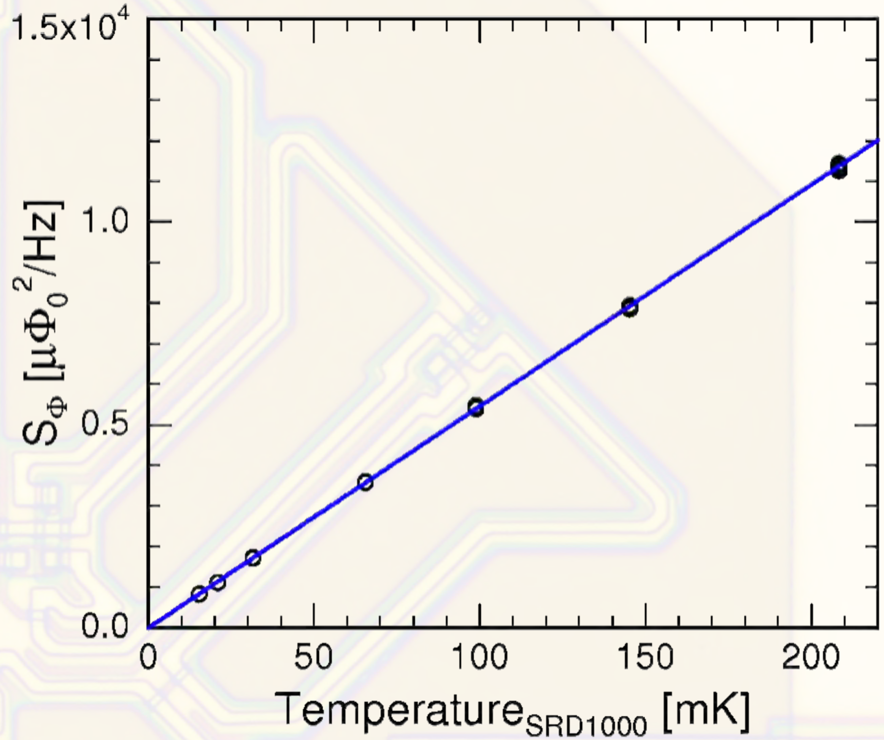

- spectral shape independent of temperature !
- SQUID noise corresponds to T_N = 150 µK
- linear temperature dependence of noise power $S_\Phi \sim T$

Thermometry at Low Temperatures

MFFT without flux transformer

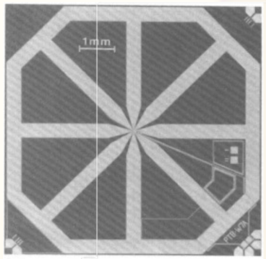

SQUID magnetometer

Circuit board

Copper noise source RRR = 100

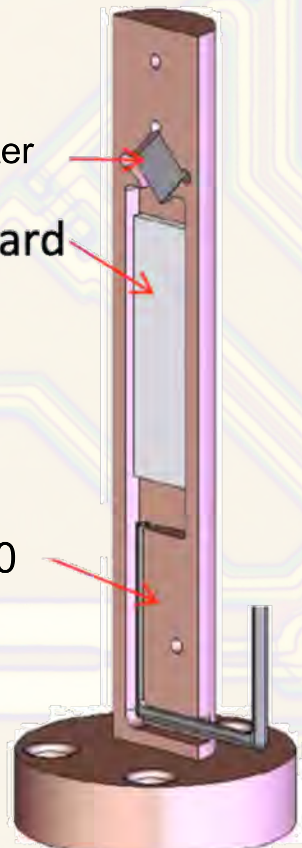

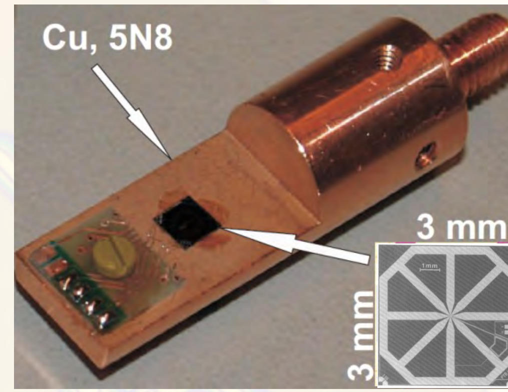

- Johnson noise is inductively read out with gradiometric waggon-wheel dc-SQUID.
- Tolerates an enormous parasitic heat load; even the dc-SQUID (100pW) can be heat sunk through the thermometer.
- Commercial version calibrated by PTB available from Magnicon

Thermometry at Low Temperatures

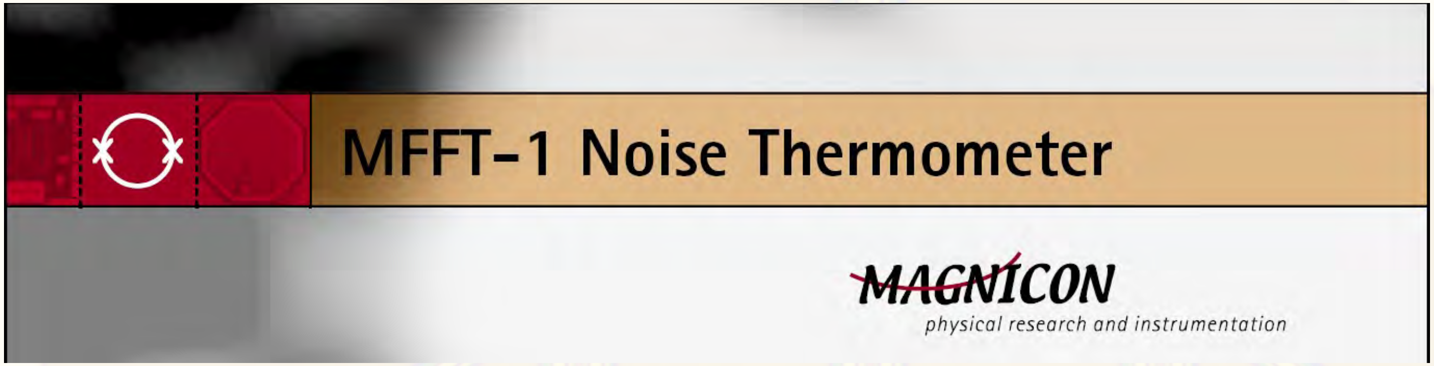

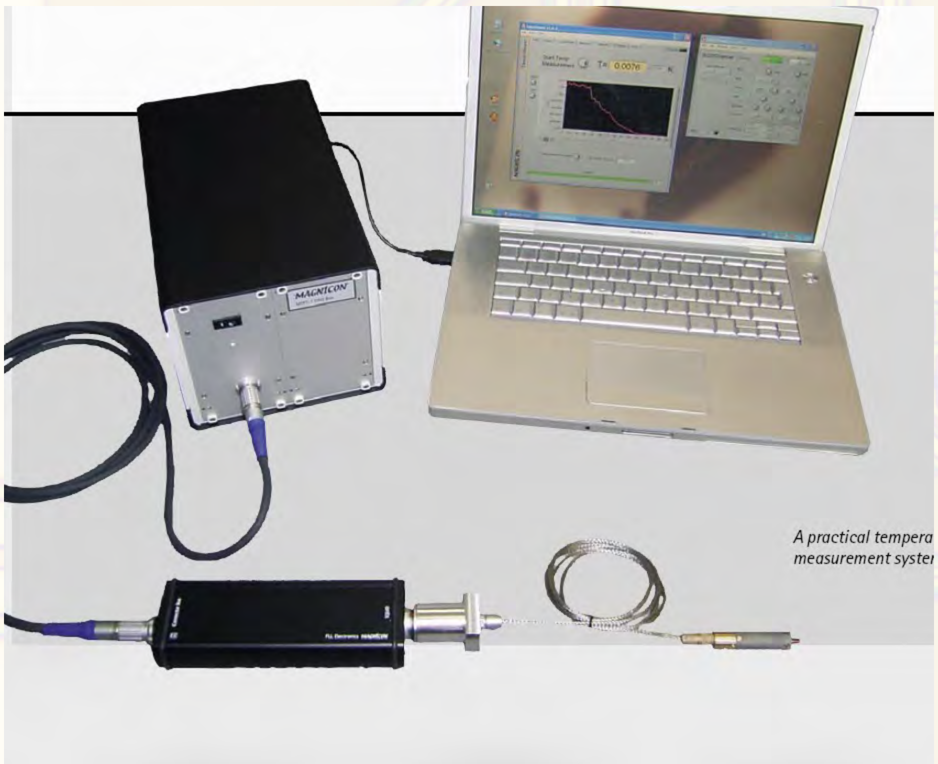

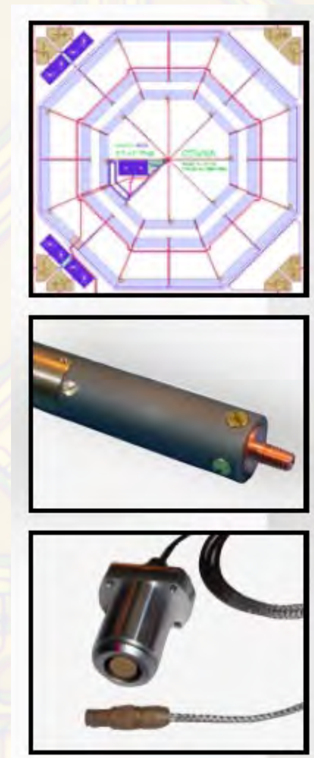

Noise thermometry at ultralow temperatures

Problem:
noise amplitudes become very small

Requirements for noise source:
high conductivity → large signal
low conductivity → wide bandwidth
constant conductivity at low temperatures

high purity copper (5N),
free of Kondo-impurities
additional heat treatment to release hydrogen
→ very high conductivity (RRR ~1000)

optimizing the RRR by cold working

→ cut-off frequency ~ 100 Hz

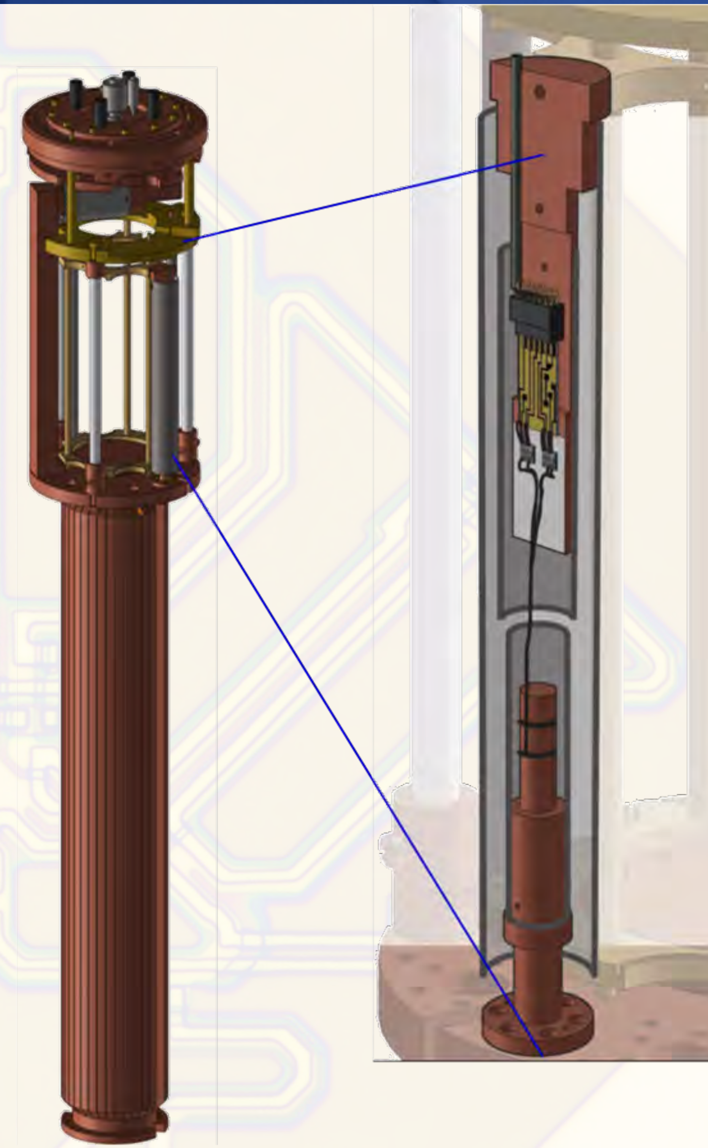

Spectral power density: after cross-correlation

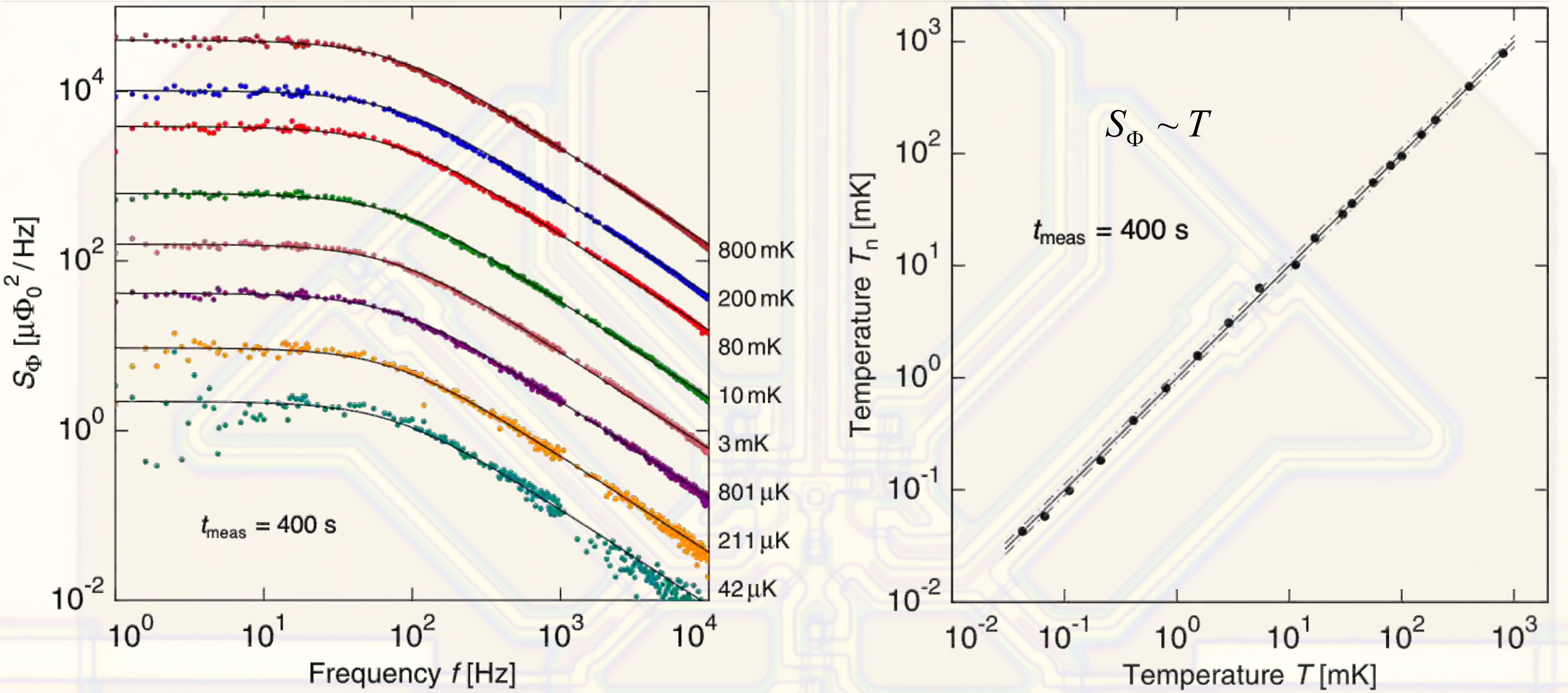

- spectral shape the same at all temperatures → R and L are constant
- spectral power density proportional to T over five orders of magnitude in temperature
- calibrated against fix point thermometer and ^{195}Pt

p-MFFT for Metrology applications

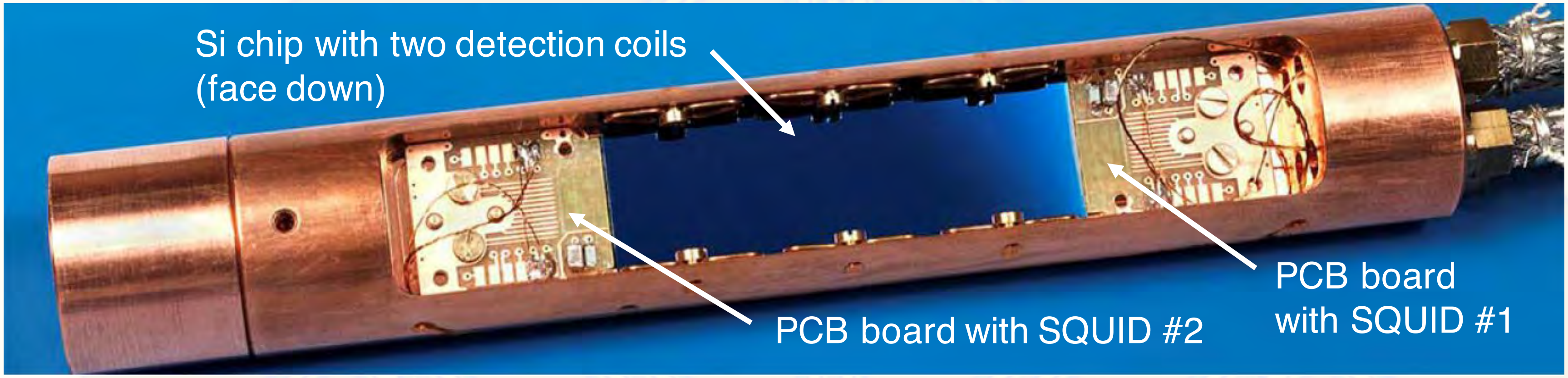

Signal calculation with result of calibrations

$$S_{12} \triangleq S_\Phi(c_1, c_2) = \mu^2 \sigma k_B T \iint_{-\infty}^{\infty} I_A e^{-\sqrt{a^2+b^2}(z_1+z_2)} \left(I_x(c_1) I_x^*(c_2) + I_y(c_1) I_y^*(c_2) \right) \mathrm{d}a \mathrm{d}b$$

with

$$I_x(c_j) = \oint_{c_j} e^{iax_j} e^{iby_j} \mathrm{d}x_j, \quad I_y(c_j) = \oint_{c_j} e^{iax_j} e^{iby_j} \mathrm{d}y_j, \quad j = 1, 2$$

$$I_A = \int_0^t |A(a,b)|^2 dz', \qquad A(a,b) = e^{-\rho' z'} (\pi \rho')^{-1} (u + v e^{-2\rho'(t-z')}) (u^2 - v^2 e^{-2\rho' t})^{-1},$$

$$\rho^2 = a^2 + b^2, \quad \rho'^2 = \rho^2 + k^2, \quad u = 1 + \frac{\rho}{\rho'}, \quad v = 1 - \frac{\rho}{\rho'}, \quad k^2 = i\mu\sigma\omega, \quad \omega = 2\pi f \; .$$

Readout and with cross-correlation and calibration scheme

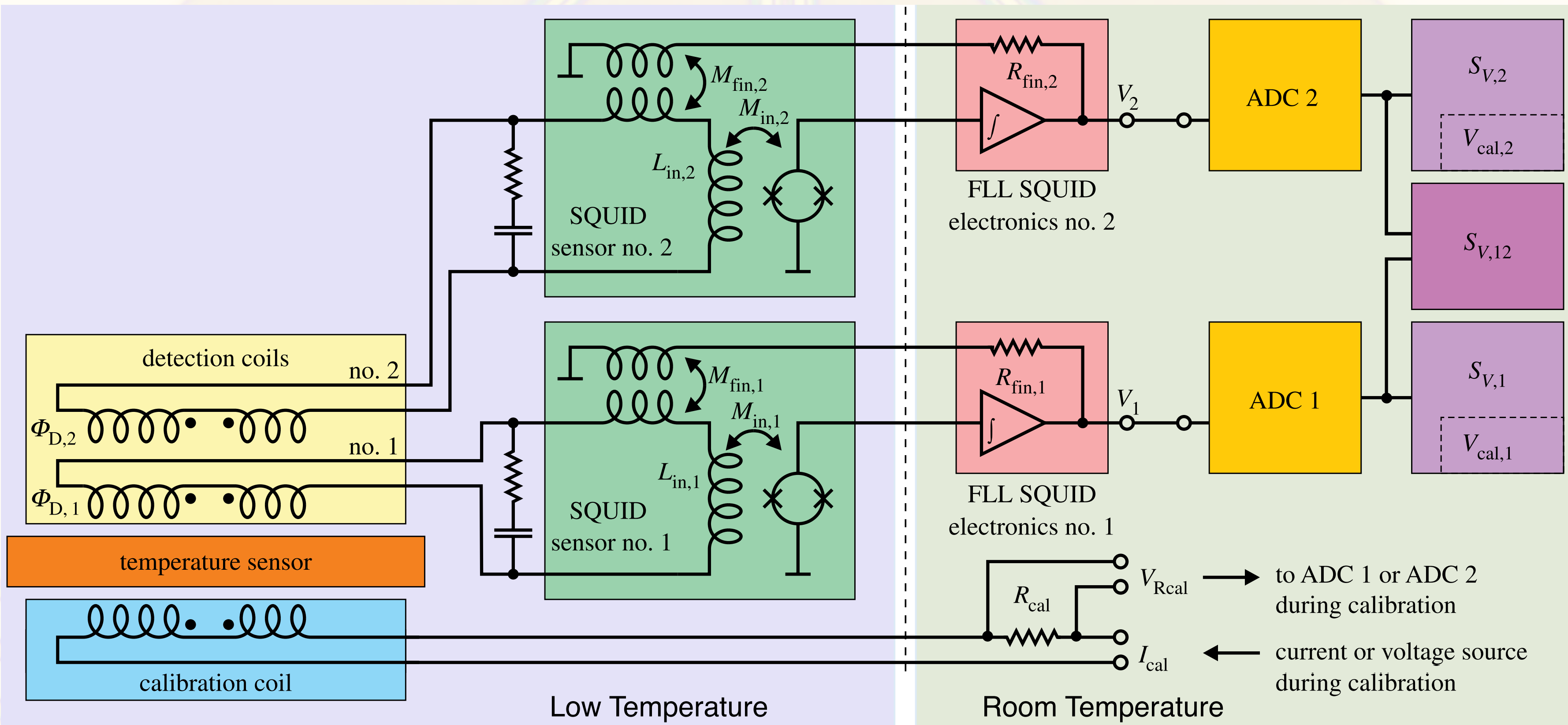

Thermometry at Low Temperatures

Noise power density vs frequency

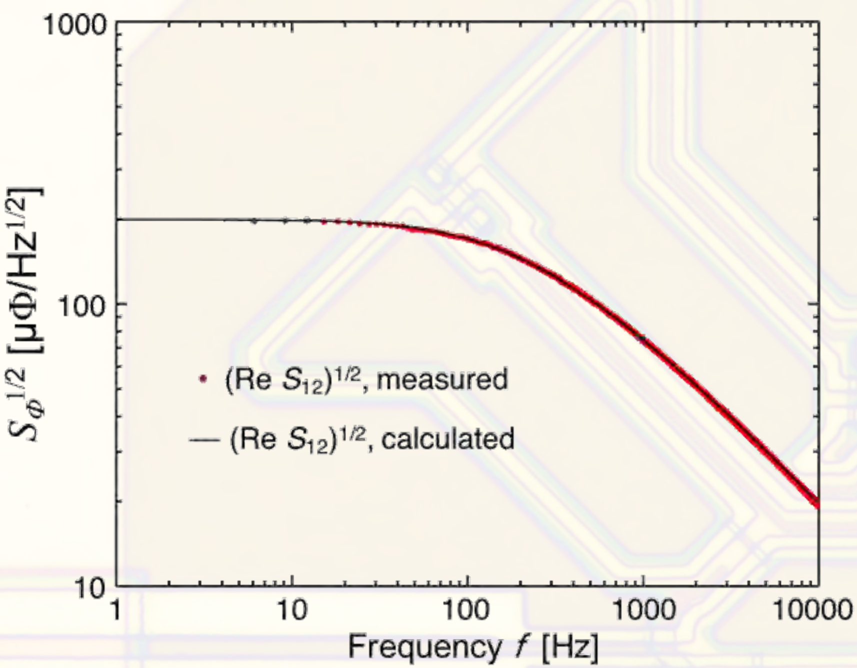

deviations between p-MFFT and PLT-2000

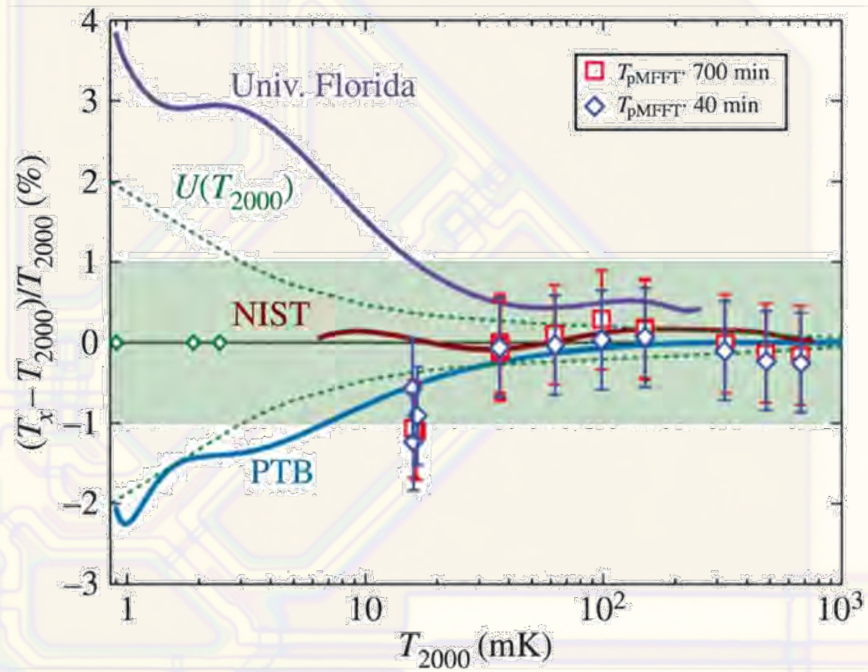

Particle Detection

- Dark matter searches
- Nuclear physics: Gamma spectroscopy
- Atomic physics: X-ray spectroscopy
- Cosmic microwave background
- Radiation metrology
- Mass spectrometry
- Neutrino mass determination

iridium thermometer. Operated at 135mK,

1.1g of silicon as absorber

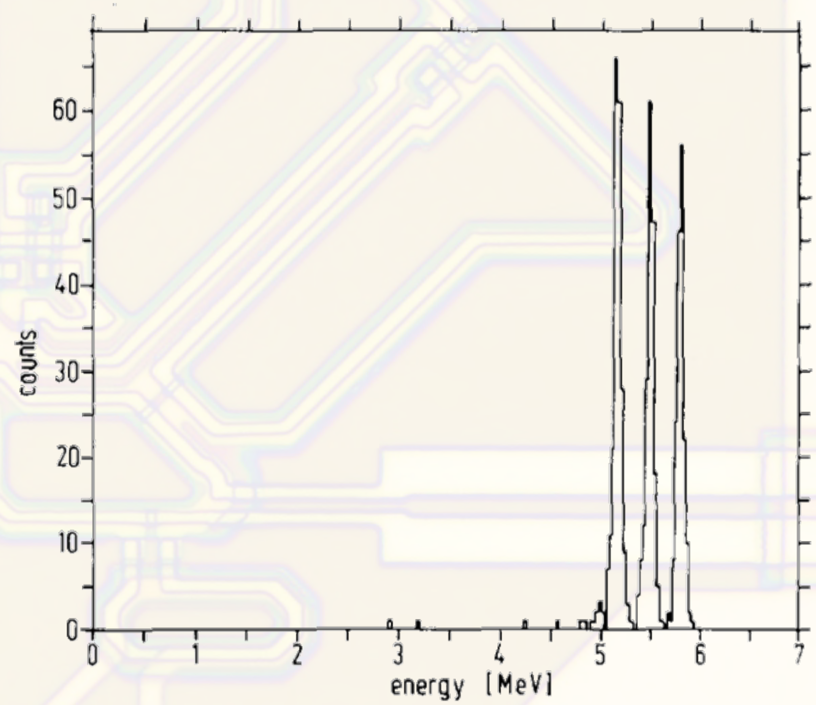

Particle Detection

First SQUID-based cryogenic particle detector 1989: Cd-TES

Transition curve

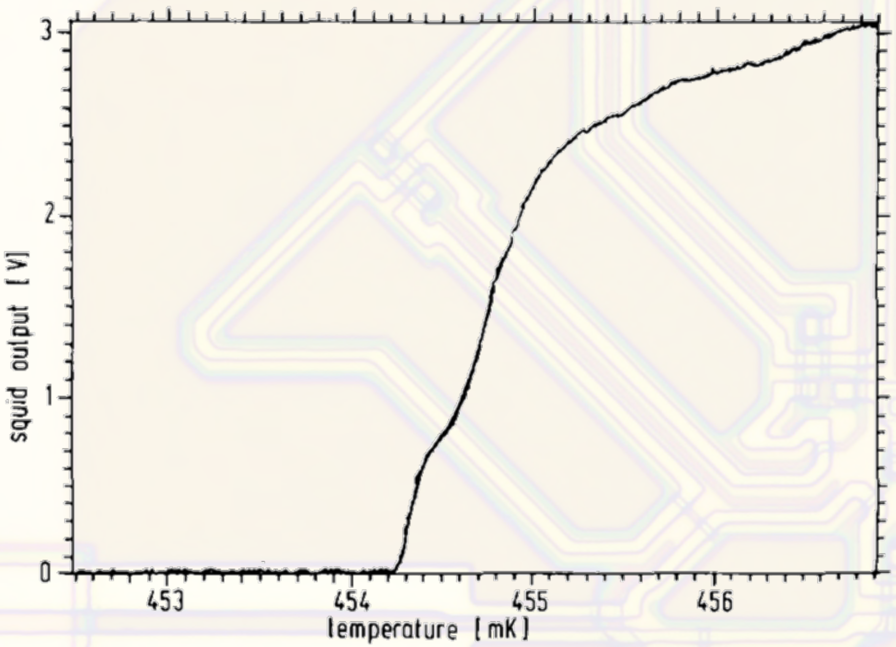

α-spectrum

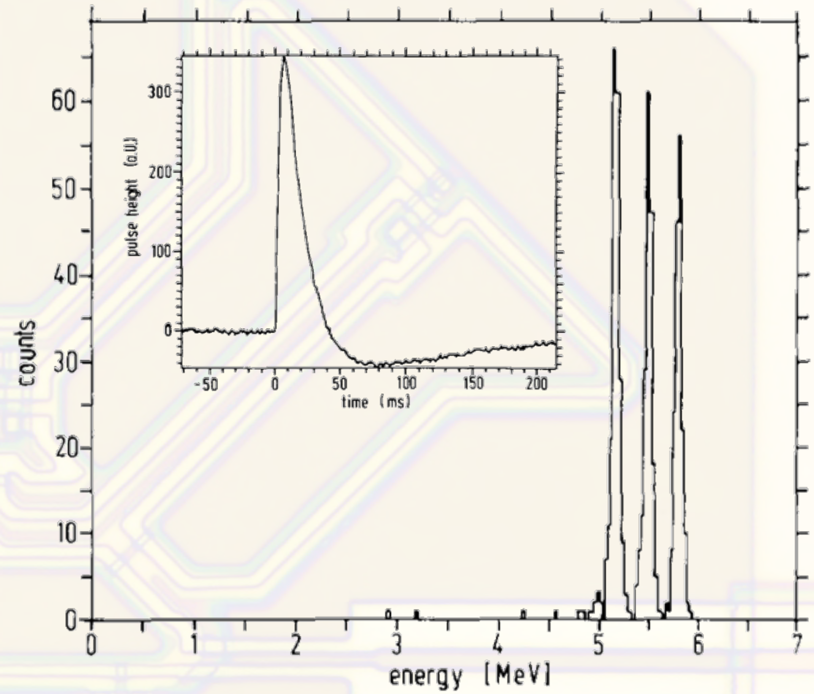

Superconducting Transition Edge Sensors (TES)

Materials Mo/Cu
Ir/Au
W

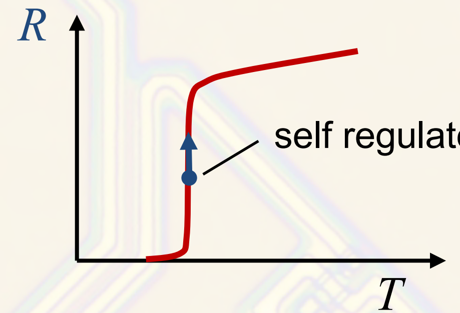

Main applications:

X-ray and γ-ray spectroscopy
CMB measurements
dark matter detection
neutrino physics
mm-wave astronomy
material analysis
...

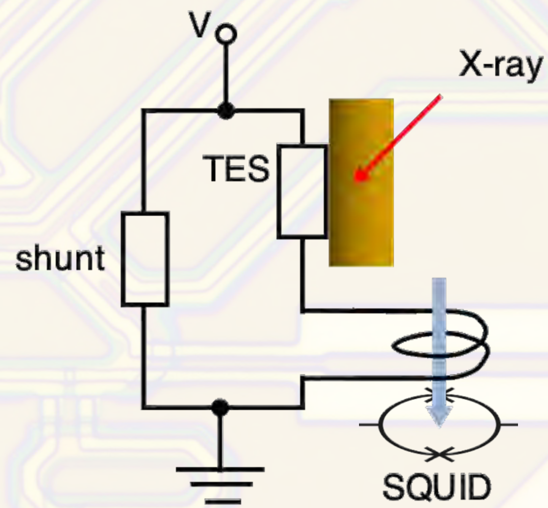

low impendence

Electrothermal feedback

equivalent circuit

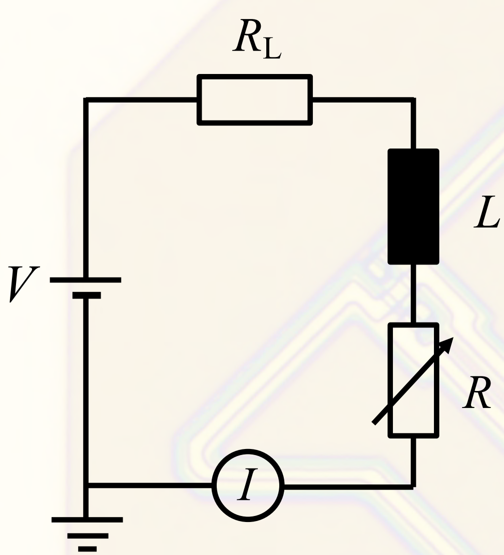

neglecting noise:

thermal differential equation

$$C\frac{\mathrm{d}T}{\mathrm{d}t} = -P_\mathrm{bath} + P_\mathrm{J} + P$$

signal power

Joule power dissipation

power flowing to bath

sensor and absorber heat capacity

electrical differential equation

$$L\frac{\mathrm{d}I}{\mathrm{d}t} = V - IR_L - IR(T,I)$$

TES resistor

load resistor

$R_L \gg R$ ⟶ $I = \mathrm{const.}$ ⟶ $P_J = I^2R$ increases ⟶ positive feedback

$R_L \ll R$ ⟶ $V = \mathrm{const.}$ ⟶ $P_J = V^2/R$ decreases ⟶ negative feedback

$R_L = R$ ⟶ no feedback

Realizations

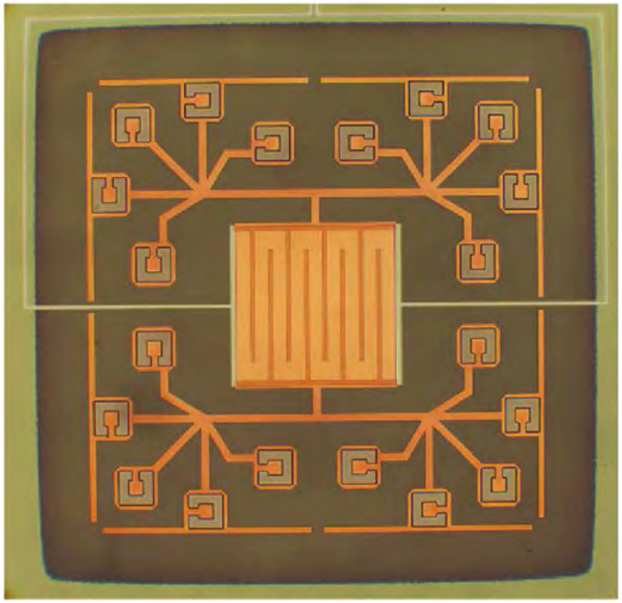

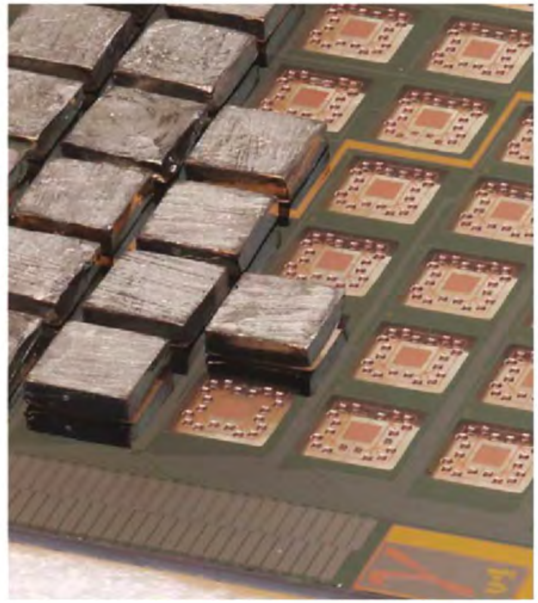

Gamma ray detector

- MoCu bilayer on SiN membrane
- tin absorber glued on stems

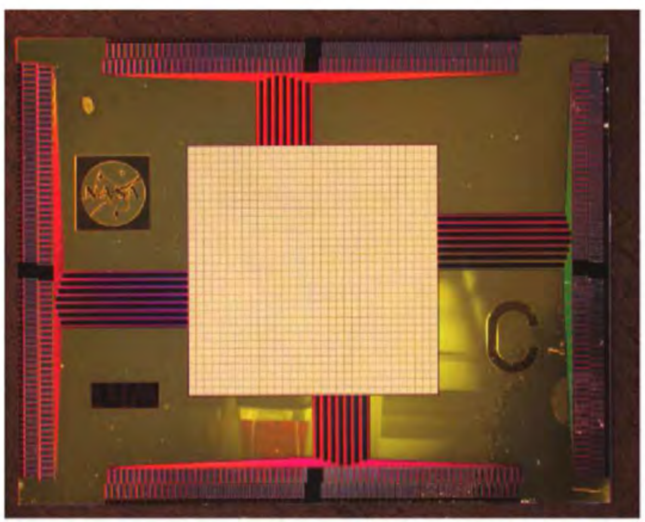

X-ray detector

- 32 x 32 array
- bismuth absorber SEM image

Performance of X-ray TES detectors

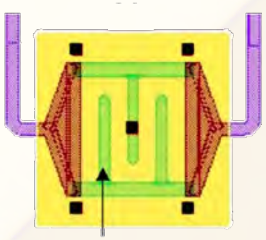

35 × 35 μm² Mo (62 nm) / Au (180 nm) bilayer

64 μm × 64 μm x 4.5 μm Au absorbers

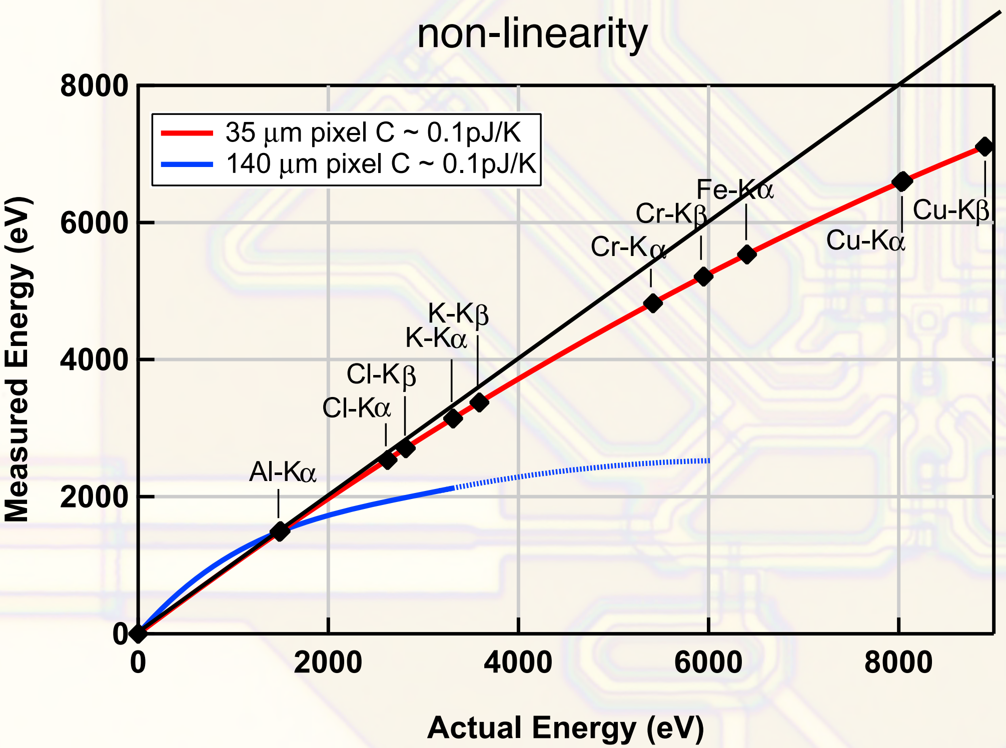

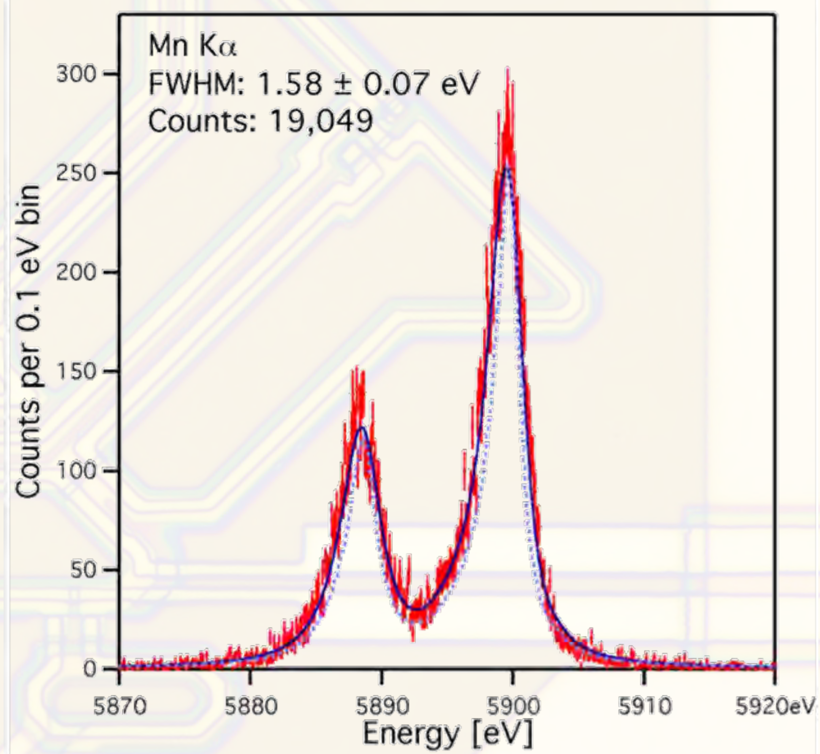

ΔE_{FWHM} = 1.58 eV at 5.9 keV